# Compact, Tunable and Narrowband Waveguide Filters Using TM Dual-Mode Cavities for Satellite Communication Applications

**Ahmadreza Eskandari**
Department of Electrical Engineering,
East Tehran Branch, Islamic Azad
University,
Tehran, Iran.
ar_eskandary@yahoo.com

**Ali Kheirdoost***
ICT research Institute of Iran
(ITRC)
Tehran, Iran.
a.kheirdoost@itrc.ac.ir

**Hadi Safdarkhani**
Electrical Engineering Department,
Yazd University,
Yazd, Iran.
safdarkhani@yazd.ac.ir

*Abstract*—**A compact, tunable and narrowband filter using dual TM mode is presented in Ku-band as a channelizing filter in IMUX of satellite transponders. To shrunken the filter structure while keeping the resonator Q a pair of degenerated modes ($TM_{120}$, $TM_{210}$) are exploited. Consequently, a single cavity capable of providing two transmission zeroes besides two poles is achieved. Later, design steps of a four-cavity filter at central frequency of 10.97 GHz with 36 MHz bandwidth are reported and also compared with the experimental results. To improve the passband flatness, chamfered corners with tuning screws are used in the second version of the fabricated filter. The results satisfy the design requirements. The agreement between full wave simulation and the experimental results demonstrates the effectiveness of the proposed design approach.**

*Keywords-tunability, tuning screws, dual-mode, transverse magnetic (TM) mode.*

## I. INTRODUCTION

DE-multiplexers sometimes referred to as IMUX in satellite communication, play the role of channelization of the received signals before amplification. Later, the dual task of combining the amplified signals (PA outputs) is done using output multiplexer or OMUX with handling high powers handling capabilities [1]. So, an IMUX is a key subsystem in payloads of communication satellites (Fig.1). It is very common to realize IMUX using narrowband bandpass filters with fractional bandwidth of about 0.2~2% [2],[3]. DR technology have been very common in IMUX realizations because of their temperature stability and also capability in size and weight reductions [4],[5]. But the DR filters are hard to be tuned and the fabrication technology sometimes becomes complicated and expensive [6],[7].

For decades, the dual-mode filters have been the optimum choice for the channel filters too thanks to their compact size and sharp selectivity, low loss and low cost [3], [8]. Conventionally, the dual-mode
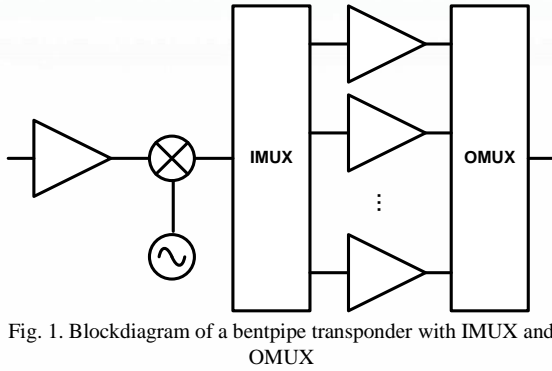
---

* Corresponding Author

Fig. 1. Blockdiagram of a bentpipe transponder with IMUX and OMUX

structures are realized using two degenerated $TE_{11n}$ modes in circular waveguide resonators [9]. The same technique can be used with different modes in rectangular waveguides, where the cross section is sized so that two degenerated $TE_{101}$ and $TE_{011}$ modes are excited [8]-[11]. Generally, most of channel filters for IMUXs are pseudo-elliptic functions, with limited number of transmission zeros. The TM dual-mode cavity has been introduced in [12] to overcome this limitation. In this design, using non-resonating modes for a cross-coupling the cavity provides two reflection and two transmission zeroes. Therefore, improved selectivity is achieved [12]-[16].

In this manuscript, design and implementation of two TM dual-mode filters are presented. Since the resonance frequency of TM modes are not dependent to the longitudinal size of the resonator, the resonator length can be chosen according to the required Q-factor. Therefore, a compact and highly selective filters are achieved. A square cavity that can produce two degenerate $TM_{mn0}$ modes, is studied in related literature and it is demonstrated that if the pair of degenerate modes resonating in these cavities, are the $TM_{120}$ and the $TM_{210}$ modes, minimum volume and maximum Q-factor will be achieved[16]. In the following, an $8^{th}$-order TM dual-mode filter is designed and fabricated to satisfy the requirements which are as follows:
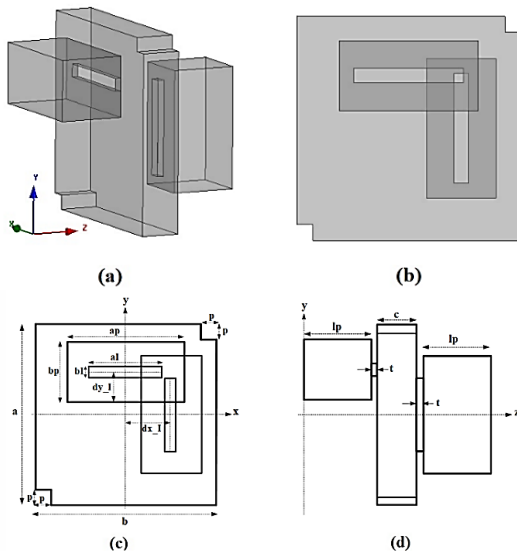


Fig. 2. Schematic of  a single cavity TM dual-mode filter: (a) Perspective view in HFSS model, (b), (c) Front view and (d) Side view of the structure [19]
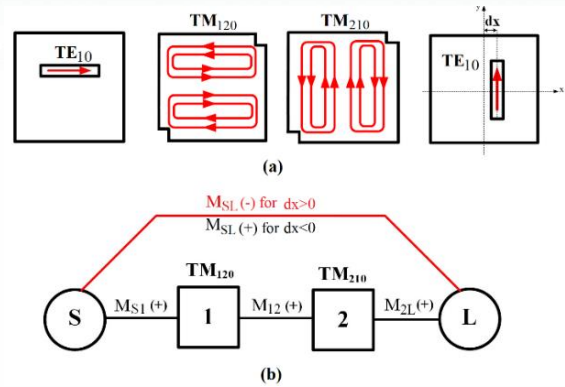


Fig. 3. Coupling mrechanism between : (a) Transverse magnetic field of the two resonance modes ($TM_{120}$, $TM_{210}$) and dominante $TE_{01}$ mode, (b) Filter topology.

$f_0 = 10970$ MHz , BW = 36 MHz , RL < -12dB , Pass-band ($f_0 \pm 18$MHz) insertion loss variations of less than 2dB , Pass-band ($f_0 \pm 18$MHz) group-delay variations of less than 60 nsec and  Stop-band ($f_0 \pm 22$MHz) of greater than 18dB.

## II.     FILTER DESIGN

The structural schematic of a TM dual-mode filter with a pair of degenerate modes ($TM_{120}$, $TM_{210}$) is shown in Fig. 2 [12]. The opposite corners of the cavity are usually stepped inside the resonator to act as intra-cavity cross coupling between degenerate modes.

TABLE I.       DUAL-MODE SINGLET OPTIMUM DIMENSIONS IN 10970MHz

| Parameters | Dimensions (mm) |
|---|---|
| In/Out Port (ap × bp × lp) | 19.05 × 9.525 × 10 |
| Cavity (a × b × c) | 30.625 × 30.625 × 8 |
| In/Out Iris (aI × bI × t) | 13.5 × 2 × 1 |
| Step Corner (p × p) | 2.45 × 2.45 |
| In/Out Offset (dx_I = dy_I) | 7.2 |

The input and output waveguides are symmetrically placed, with s displacement of dx_I and dy_I as shown in Fig. 2(c). Such structure known as singlet can produce two poles and two transmission zeroes due to using non-resonating modes to implement a cross-coupling. Fig. 2 shows the full geometry of the singlet structure using two degenerated TM modes from different views and various parameters. The coupling mechanism between the dominant electric $TE_{01}$ mode of the waveguide feeds and the magnetic modes inside the cavity is shown in Fig. 3.
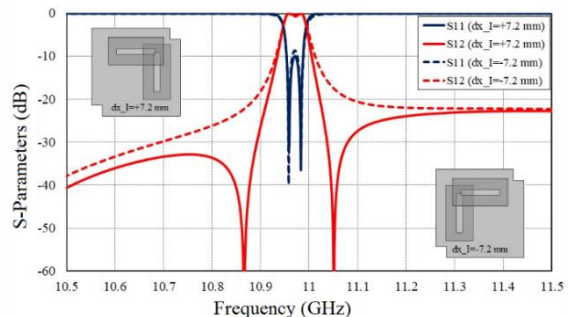


Fig. 4. HFSS simulation of the 10970-MHz TM dual-mode single-cavity filter with two different position of the input and output ports respect to the resonator stepped corners.
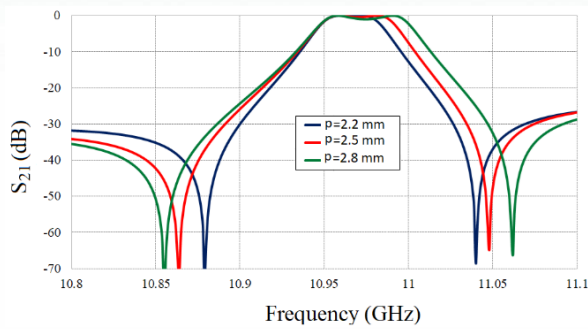
Fig. 5. The effect of p parameter of frequency response of the singlet and the transmission zeros (p=2.2, 2.5, and 2.8 mm).
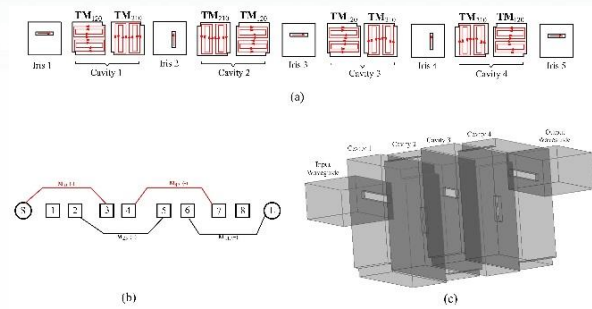


Fig. 6. Order 8 TM dual-mode filter with four cavities: (a) the layout of the cross-sectional magnetic field distributions, (b) topology, (c) filter structure.

The sign of the $M_{SL}$ coupling is determined by the relative position of the input and output ports respect to the stepped corners of the cavities as shown in Fig. 3 (b). In this paper, the full-wave EM simulations of TM dual-mode filters with single cavity or more are performed using HFSS. Also all of the optimum values extracted from the simulations are reported in TABLE I. Fig. 4 also shows the HFSS simulation of the optimized single-cavity filter. As is clear, the optimal frequency responses are obtained when the input and output irises are properly placed respect to the cavity center. The bandwidth and transmission zero frequency can be properly tuned by adjusting the p parameter. Fig. 5 shows the effect of adjusting the p parameter on the frequency response of the filter.

## III.        REALIZATION AND EXPERIMENTAL RESULTS

### A.        The first version of fabricated filter

To meet the requirements specified in section I, an order 8 filter using four TM dual-mode cavities is realized by applying the principles and concepts of the literature [12]. The coupling between the cavities is also realized using thin slot shaped irises as used in [17], [18]. To show the operation concept of the filter coupling, the cross-sectional magnetic field distributions for the cavities are shown in Fig. 6(a). This arrangement is named as singlet and generates two pairs of transmission zeroes. Also, the designed filter can be properly described by the coupling scheme in Fig. 6(b). In this topology, weak coupling lines (as for: MS5, MS7, MSL, M27, M2L and M4L) are not drawn, also the lines with negative coupling are drawn in red.

The final structure of the designed by extending this concept to design a filter (HFSS model) is depicted in Fig. 6(c). TABLE II lists all the filter optimized dimensions. The cavity lengths of 10 mm is selected based on the discussion presented in [16]. The filter has been manufactured using silver coated aluminum parts. The components have been stacked together, and the measured prototype of the filter is depicted in Fig. 7. The total filter length, excluding the feeding waveguide (WR-75) flanges, is 41 mm. The unloaded Q factor is estimated to be about 5800, based on the measurements [19]. As the tuning screw is inserted into the resonator, the resonance frequency of the resonator is increased making the tuning process possible.

TABLE II.        FIRST FILTER OPTIMIZED DIMENSIONS

| Section Name | Dimension Parameters | Values (mm) |
|---|---|---|
| In/Out Waveguide (WR75) | ap × bp × lp | 19.05 × 9.53 × 15 |
| Iris 1 | aI1 × bI1 × t1 | 12.53 × 2.05 × 1 |
| Iris 1 offset | (dx_I1 , dy_I1) | (0.15 , 6.32) |
| Fist Cavity | a1 × b1 × c1 | 30.49 × 30.64 × 10 |
| Iris 2 | aI2 × bI2 × t2 | 2.21 × 6.94 × 1 |
| Iris 2 offset | (dx_I2 , dy_I2) | (4.52 , 0.08) |
| 2nd Cavity | a2 × b2 × c2 | 30.52 × 30.54 × 10 |
| Iris 3 | aI3 × bI3 × t3 | 7.25 × 2.18 × 1 |
| Iris 3 offset | (dx_I3 , dy_I3) | (0.08 , 5.41) |
| 3rd Cavity | a3 × b3 × c3 | 30.53 × 30.53 × 10 |
| Iris 4 | aI4 × bI4 × t4 | 2.30 × 6.23 × 1 |
| Iris 4 offset | (dx_I4 , dy_I4) | (5.03 , 0.03) |
| 4th Cavity | a4 × b4 × c4 | 30.48 × 30.66 × 10 |
| Iris 5 | aI5 × bI5 × t5 | 12.61 × 2.11 × 1 |
| Iris 5 offset | (dx_I5 , dy_I5) | (-0.12 , 6.23) |
| Stepped corners | p1=p4 p2=p3 | 2.61 2.42 |

The agreement between the measurement and simulation results has been obtained after a little tuning involving only the cavity resonance frequencies: to this purpose, a pair of orthogonal screws has been inserted into each cavity. Insomuch the screws are located at the peak of the magnetic field; the resonance frequencies increase with the screw penetration.

The comparison between the simulation and measurement results are presented in Fig. 8 and Fig. 9. Specifications of these results are reported in table III. Acceptable agreement between the measurement and simulation results makes the design promising.

TABLE III.        MEASURED FREQUENCY RESPONSE THE FIRST FILTER

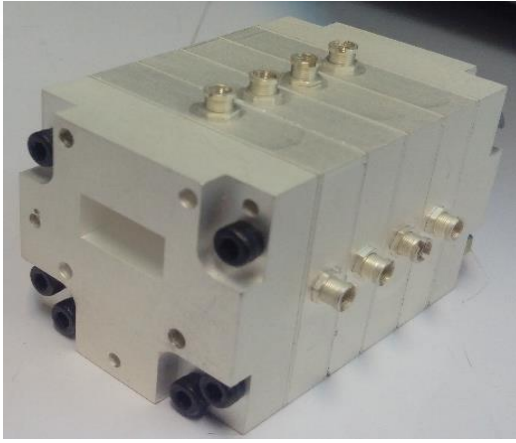| Items | Value |
|---|---|
| Central Frequency ($f_c$) | 10.970 GHz |
| Bandwidth (B.W.) | 36 MHz |
| Passband Insertion Loss @ $f_c$ | 1.5 dB  (Sim.) 2.1 dB  (Meas.) |
| Returne Loss | > 15 dB (Sim.) > 13 dB (Meas.) |
| Out of Band Rejection ($f_c$ ± 22 MHz) | 19.5 dB (Sim.) 20.3 dB  (Meas.) |
| Amplitude Variation ($f_c$ ± 18 MHz) | 2 dB   (Sim.) 2.2 dB  (Meas.) |
| GD Variation ($f_c$ ± 18 MHz) | 65 ns (Sim.) 62 ns (Meas.) |

Fig. 7. Picture of the first fabricated filter.

### B. The second version of the fabricated filter: with tunable cross coupling screws

Amplitude variation or passband flatness reported in the measured results (Table III) does not satisfy the requirements specified in the section I and needs to be improved. Since the design is accurate enough but there are some differences between the design simulation and measurement, other than the resonance frequency of the resonators, the couplings needs to be tuned. So this improvement is realized using tunable coupling tools. As mentioned in the previous section, the coupling between the modes of the cavities were realized using thin irises, while, intra-cavity cross coupling between the degenerated modes were realized with stepped corners. Since the corners were not tunable, the cross coupling between the modes using the previous technique is fixed. So in this section a technique is
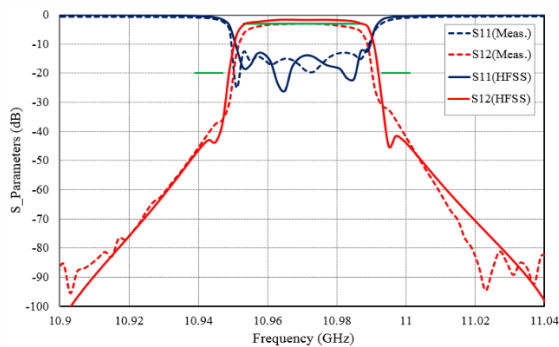

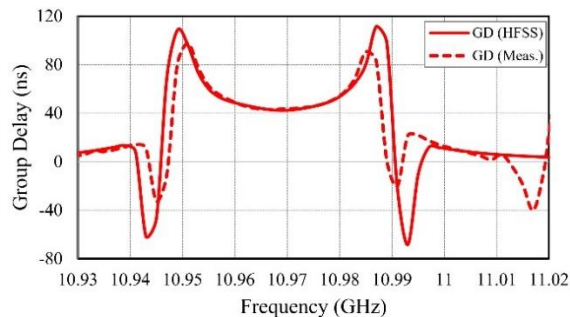Fig. 8. Measurement and full-wave simulation of the order 8 TM dual-mode filter in 10970 MHz.


Fig. 9. Measurement and full-wave simulation of the GD frequency response for the order 8 TM dual-mode filter in 10970 MHz.

proposed to tune the intra-cavity couplings in order

to improve the passband flatness. The proposed structure is shown in Fig. 10. In this structure, intra-cavity couplings between degenerated modes are all realized with cavity chamfers (pxp) replaced with the stepped corners. The screws located at 45º (within the chamfers) can simplify the tuning process as well as the improvement in the amplitude variation. The final structure (HFSS model) of the proposed filter with chamfered corners and coupling screws for tuning of the intra cavity cross coupling is depicted in Fig. 11. The optimized dimensions (pxp) of the chamfer corners for each of the cavity are presented in Table IV. The second version of this filter with chamfered corners and coupling screws has been fabricated and tested. The picture of this fabricated filter is shown in Fig. 12. The fabrication process in this structure was done using CNC machining which resulted in better surface roughness. The sharp square corners in the previous version required wire cut fabrication process which usually results in degraded surface roughness compared to CNC machining process. So in the second version of the fabricated filter, beside the tunability improved surface roughness is also achieved. The simulation and measurement results of this second version are compared and presented in Fig. 13 and Fig. 14.

TABLE IV. OPTIMIZED DIMENSIONS OF THE CHAMFER CORNERS

| Chamfered corners | Parameters | Values (mm) |
|---|---|---|
| For cavity 1 | P1×p1 | 3.75×3.75 |
| For cavity 2 | P2×p2 | 3.20×3.20 |
| For cavity 3 | P3×p3 | 3.15×3.15 |
| For cavity 4 | P4×p4 | 3.72×3.72 |

During the mechanical and EM design and optimization process it should always be considered that the chamfer length of p has to be adequately more than the tuning screw diameter. Also the tuning screw lock mechanism using nuts, needs to be accounted for in mechanical design of the structure.

In Fig.13, the measurement results have been obtained after the tuning using the resonance and coupling tuning screws. Significant improvement of the amplitude variation is observed in this measurement compared to the first version.
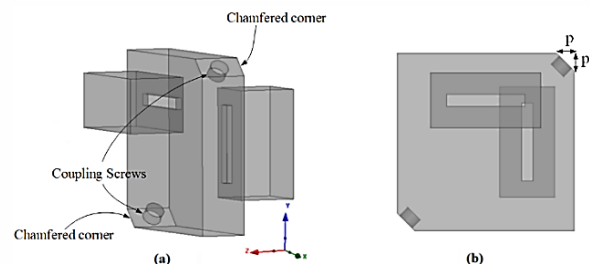

Fig. 10. Proposed structrue with chamfered corners and coupling screws: (a) Perspective view in HFSS model, (b) Front view.
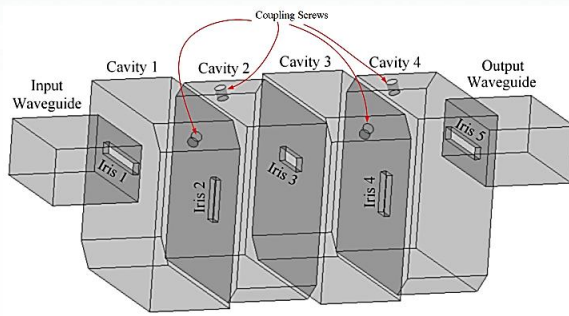
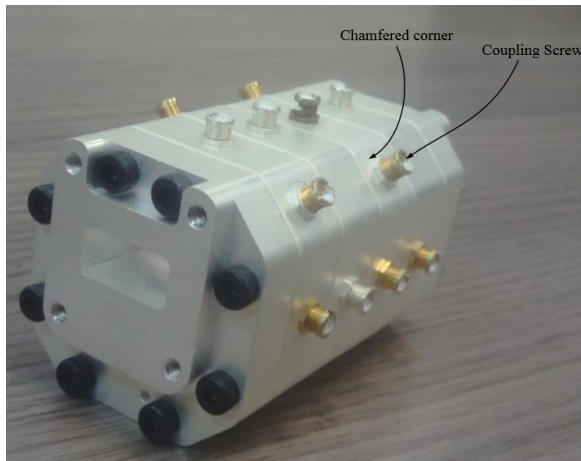Fig. 11. Filter structure with chamfered corners and coupling screws.



Fig. 12. Picture of the fabricated filer with chamfered corners and coupling screws.

At the lack of this step, it could be misinterpreted that the degradation in quality factor of the resonator have resulted in rounded corners in the passband frequency response of the Fig. 8.
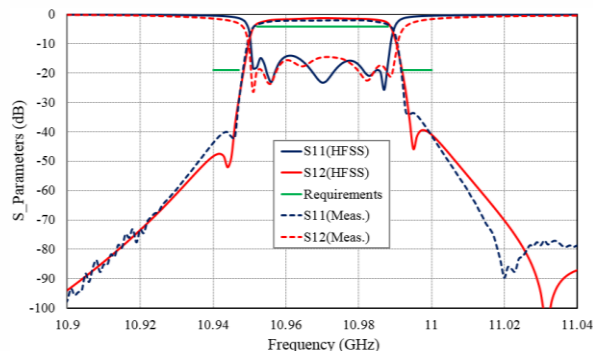


Fig. 13. Measurement and full-wave simulation of the four-cavity TM dual-mode filter (with tunable coupling screws).
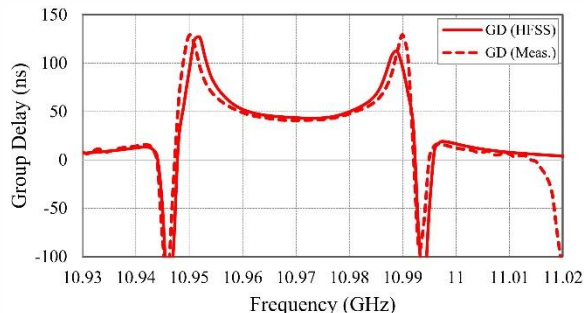


Fig. 14. Measurement and full-wave simulation of the GD frequency response for 4-cavity TM dual-mode filter (with tunable coupling screws).
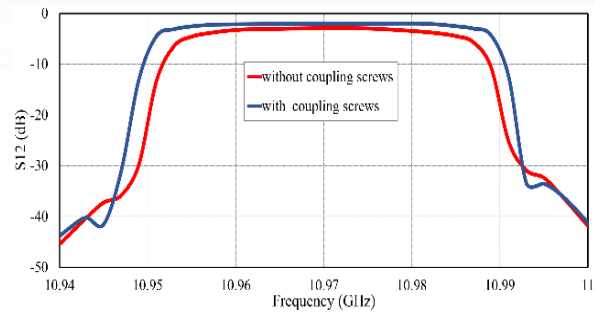


Fig. 15. Comparison of the measurements for the fabricated filters with and without coupling screws.

TABLE V. SPECIFICATIONS OF THE MEASURED IN-BAND RESPONSE

| Parameters | Without coupling screws | With coupling screws |
|---|---|---|
| Insertion Loss @ $f_c$ | 2.1 dB | 2.08 dB |
| Amplitude Variation ($f_c \pm 18$ MHz) | 2.2 dB | 1.49 dB |
| Amplitude Variation ($f_c \pm 18$ MHz) | 62 ns | 55 ns |

This step proves that the possibility of the tuning of the inter-cavity coupling tuning can also play a role in frequency response enhancement which is not physically feasible in this realization. Comparison of the measurements for the fabricated filters with and without the cross coupling tuning screws are presented in the Fig. 15.

As shown in figure 15 and TABLE V, the amplitude variation has been improved from 2.2 dB to 1.49 dB by invoking the tuning screws in the cross couplings. Improvement in matching of the input and output ports of the measurements (Fig.8 and Fig.13 comparison) is noticeable too.

It was also experienced that using the cross coupling tuning screw, the bandwidth of the filter can be partially tuned which was a key step in reaching the frequency response requirements. By adjusting the bandwidth of the filter beside the input/output ports matching and passband flatness, the tuning of the out of band rejection in frequency response of the filter was also possible. This step is a critical need in using the narrowband filters in contagious multichannel IMUX or OMUXs in which the rejection response of the adjacent channel happens in the passband edge of the other channel and consequently the sharp rejection response plays a key role. In most of the contiguous applications including the adjacent channel in design is not adequate and it is necessary to tune the out of band rejection response too which results in a trade off in passband edge and adjacent channel out of band rejection response. During the tuning of the frequency response, trial and error was the main method for fine tuning of the frequency response, while during the coarse tuning other technique like group delay technique was also invoked which is discussed in literature in depth [20]. The better agreement between the simulation and measurement results of the group

delay is also another key advantage of the second version compared to the first version. In practical application of the IMUX, input group delay performance of the filters play a key role in distortion specification of the signals passing through the TWTAs after being channelized by IMUX, specifically in phase modulation which are very common in satellite communication standards like DVB-S/S2. So the group delay performance of the IMUX filters have to be tuned and compensated precisely to avoid any adverse effects coming from the TWTAs nonlinear performance. Using the cross coupling tuning screws was also helpful in reaching such goal. The group delay response and compensation of the designed and fabricated filter is also discussed more details in [16]. The group delay equalizers used in [16], compensates the group delay and amplitude variations simultaneously.

## IV. CONCLUSION

A new dual mode waveguide filter using TM mode cavities has been presented for the realization of a compact, tunable, narrowband and high Q channel filter in IMUX of a satellite transponder. Two order 8 TM dual mode filters in 10.97-GHz with FBW=0.33% are designed, fabricated and tested. Amplitude flatness of 2.2 dB and 1.49 dB in the passband with high rejection at the out-of-band are reported. It was proved that the intra cavity cross coupling tuning screw play a key role in pass band response enhancement as well as the bandwidth and out of band rejection response which is an essential need for multi-channel IMUX and OMUX applications. The physical architecture of the fabricated filters are compact, highly-selective, tunable and also insensitive to longitudinal size of the resonators. Even though in both designs, measurements show a good agreement with the full-wave HFSS simulations in both designs, the strict system requirements were the main motivation for improved design and better response consequently.

## REFERENCES

[1] V.E. Boria and B. Gimeno, "Waveguide Filter for Satellite," *IEEE Microwave Magazine*, Vol. 8, No. 5, pp. 60-70, Oct. 2007.

[2] Richard J. Cameron and Ming Yu, "Design of Manifold-Coupled Multiplexers", *IEEE Microwave Magazine*, Vol. 8, No. 5, pp. 46-59, Oct. 2007.

[3] Hai Hu, Ke-Li Wu, and R.J. Cameron, "Stepped Circular Waveguide Dual-Mode Filters for Broadband Contiguous Multiplexers", *IEEE Transactions on Microwave Theory and Techniques*, Vol. 61, No. 1, pp. 139-145, Jan. 2013.

[4] K.A. Zaki and A.E. Atia, "Modes in dielectric loaded waveguides and resonators," IEEE Trans. Microwave Theory Tech., vol. MTT-31, no.12, pp.1039-1045, Dec. 1983.

[5] O. Ozan Ozturk, S. Oruc, B. Alicioglu, and N. Yildirim, "Design of Selective Linear Phase Cross-Coupled Dielectric Resonator Filters", 2018 18th Mediterranean Microwave Symposium (MMS), pp. 218-220, 2018.

[6] Raafat R. Mansour, "High-Q tunable dielectric resonator filters," IEEE Microwave Magazine, Vol. 10, Issue 6, pp. 84-98, Oct. 2009.

[7] Z. Lei, Q. Guo, Z. Liu, J. Jiang, T. Zhang, "Design of Dielectric Resonator Cavity Filter with Double-CT to Control TZs," IEEE International Conference on Circuits, Devices and Systems, 2017.

[8] S. Amari and U. Rosenberg, "Design of dual-mode bandpass waveguide elliptic filters for simple fabrication by milling", *Int. J RF and Microwave Comp Aid Eng.*, Vol. 17, pp. 34-40, 2007.

[9] A. E. Williams, "A four-cavity elliptic waveguide filter," *IEEE Trans. Microw. Theory Tech.*, vol. MTT-18, no. 12, pp. 1109–1114, Dec. 1970.

[10] A. E. Atia and A. E. Williams, "New types of waveguide bandpass filters for satellite transponders", *COMSAT Tech. Rev.*, vol. 1, no. 1, Fall, 1971.

[11] I. C. Hunter, L. Billonet, B. Jarry, and P. Guillon, "Microwave filters Applications and technology," IEEE Trans. Microw. Theory Tech., vol. 50, no. 3, pp. 794–805, Mar. 2002.

[12] S. Bastioli, C. Tomassoni, and R. Sorrentino, "A new class of waveguide dual-mode filters using TM and nonresonating modes," IEEE Trans. Microw. Theory Tech., vol. 58, no. 12, pp. 3909–3917, Dec. 2010.

[13] S. Bastioli, L. Marcaccioli, C. Tomassoni, and R. Sorrentino, "Ultracompact highly-selective dual-mode pseudoelliptic filters," IET Electron.Lett., vol. 46, no. 2, pp. 147–149, Jan. 2010.

[14] C. Tomassoni, S. Bastioli, and R. Sorrentino, "Generalized TM Dual-Mode Cavity Filters", IEEE Transactions on Microwave Theory and Techniques, vol.59, No.12, pp.3338-3346, Dec. 2011.

[15] S. Bastioli, C. Tomassoni, and R. Sorrentino, "TM dual-mode pseudoelliptic filters using nonresonating modes", Microwave Symposium Digest (MTT), 2010 IEEE MTT-S International, July 2010.

[16] A. R. Eskandari, A. Kheirdoost and M. Haghparast, "Improvement of Passband Flatness for a Compact, Narrowband, and Highly Selective TM Dual-Mode Filter," in IEEE Transactions on Microwave Theory and Techniques, 2020.

[17] U. Rosenberg, S. Amari, and J. Bornemann, "Inline -mode filters with high design flexibility by utilizing bypass couplings of nonresonating modes," IEEE Trans. Microw. Theory Tech., vol. 51, no. 6, pp. 1735–1742, Jun. 2003.

[18] A.R. Eskandari, "Compact and Narrow-Band Waveguide Dual-Mode Filters for Output Multiplexer in Communication Satellites", *Journal of Electrical Engineering & Technology*, 14 (6), pp. 2421-2426, 2019.

[19] A. Eskandari and A. Kheirdoost, "Compact and Narrow-Band Waveguide Filters Using TM Dual-Mode Cavities for Input Multiplexer in Communication Satellites," *2020 10th International Symposium on Telecommunications (IST)*, Tehran, Iran, 2020, pp. 234-239

[20] Cameron, Richard J., Chandra M. Kudsia, and Raafat R. Mansour. *Microwave filters for communication systems: fundamentals, design, and applications*. John Wiley & Sons, 2018.

**Ahmadreza Eskandari** received B.Sc. and M.Sc. degrees in electrical engineering from Sharif University of Technology, Tehran, Iran, in 2002 and 2005, respectively, and the Ph.D. degree in electrical engineering from the Science and Research Branch, Islamic Azad University, Tehran Iran, in 2012. He is currently an Assistant Professor with the Department of Electrical Engineering, East Tehran Branch, Islamic Azad University, Tehran, Iran. His research interests are Satellite Communication Systems, Inverse Scattering in Electromagnetics, and Design of Antenna and Microwave Components.

**Ali Kheirdoost** received the B.Sc. degree in electrical engineering from the Amirkabir University of Technology, the M.S. degree in electrical engineering from the Sharif University of Technology, and the Ph.D. degree in electrical engineering from the Amirkabir University of Technology in 2005, 2007, and 2014, respectively. He joined the University of Tennessee as a Visiting Student in 2013 and is currently an Assistant Professor with the Communication Technology Research Institute of Iran ICT Research Institute (ITRC), Tehran. His research interests are UWB Systems, Microwave Nonlinear Circuits, Power Amplifiers, and Microwave Filters.

**Hadi Safdarkhani** received B.Sc, M.Sc. and Ph.D. degrees in electrical engineering from Amirkabir University of Technology, Tehran, Iran, in 2005, 2008 and 2015 respectively. He is currently an Assistant Professor with the Department of Electrical Engineering, Yazd University, Yazd, Iran. His research interests are Analog and Digital system Analysis and Design.